Temperature-dependent performance scales with maximum heat tolerance across ectotherms

Amanda S. Cicchino, amanda.cicchino@uoguelph.ca, 1,2, correspondence

Jessica Collier, jcolli15@uoguelph.ca,2

Carling Bieg, cbieg@uoguelph.ca, 1,2, 3 *

Kaleigh Davis, kaleigh.davis@uoguelph.ca,1,2 *

Cameron K. Ghalambor, cameron.ghalambor@ntnu.no,4 *

Alison J. Robey, alison.robey@yale.edu, 5 *

Jennifer Sunday, jennifer.sunday@mcgill.ca,6 *

David Vasseur, david.vasseur@yale.edu,5 *

Joey R. Bernhardt, joey.bernhardt@uoguelph.ca, 1,2

Affiliations:

1. Centre for Ecosystem Management, University of Guelph
2. Department of Integrative Biology, University of Guelph
3. Department of Biology, Case Western Reserve University
4. Department of Biology, Norwegian University of Science and Technology
5. Department of Ecology and Evolutionary Biology, Yale University
6. Department of Biology, McGill University

* These authors contributed equally and are listed in alphabetical order

Abstract

Projecting species' responses to changing temperatures remains a major challenge in ecology. Central to this effort is harnessing our understanding of species' thermal physiological traits, which underlie ectotherm fitness. These traits are typically characterized by describing performance across temperatures (thermal performance curve, TPC), and/or tolerance limits, which capture endpoints of biological failure. Despite their importance, we still lack an understanding of the functional relationship between these traits, limiting our ability to integrate them into comprehensive vulnerability assessments. Using a synthesized dataset of >100 ectotherms, we tested how tolerance (CTmax) relates to key TPC traits: thermal optima, thermal maxima, and the supra-optimal range of temperatures where performance is positive. Across taxa, TPC traits were positively related to CTmax, demonstrating a link between heat tolerance and temperature-dependent performance at sub-critical temperatures. While acute locomotor performance scaled proportionally with CTmax, metabolic processes and sustained locomotion scaled sub-proportionally, suggesting decoupling of CTmax and performance among high-CTmax species. This suggests that using CTmax as a comparative metric may overestimate thermal safety margins for metabolic processes critical to growth. Our results indicate that while CTmax and TPCs reflect shared underlying constraints—particularly in acute neuro-muscular traits—their relationship is dependent on timescale and the TPC response trait. Our findings connect our understanding of the processes that maintain performance over thermal gradients with those that cause performance to fail, improving our ability to project species persistence in a warming world.

Keywords: thermal tolerance, CTmax, thermal performance curve (TPC), supra-optimal range, ectotherm, climate warming

Significance

Climate warming is increasingly reshaping the thermal environments that govern species persistence worldwide. Predicting vulnerability requires integrating multiple aspects of thermal biology, yet relationships among widely used thermal traits remain poorly understood. By synthesizing data from more than 100 ectotherm species, we quantify links between acute heat tolerance and traits describing sustained biological function across temperatures. We show that performance at relatively benign temperatures and performance at thermal extremes are coupled, but this coupling is strongly process and timescale dependent, with close correspondence for short term locomotion but weak coupling for metabolic processes. Our results link the processes that maintain performance across temperatures with those that cause failure, fundamentally advancing our projections of species performance in a warming world.

Introduction

For the vast majority of Earth's species—the ectotherms—temperature fundamentally underlies biochemical, cellular, and physiological processes that shape fitness and population growth (1–4). As such, thermally sensitive traits have long been central to understanding the ecology and evolution of ectotherms (5, 6) and are increasingly used to predict species' vulnerability to warming by relating trait variation to current and projected habitat temperature (e.g.,(7–15)). Two commonly used experimental approaches to quantify biological responses to temperature include estimating thermal performance curves (TPCs) and thermal tolerance limits (Figure 1). While TPCs describe performance across the range of sublethal temperatures (7–9), thermal tolerance limits represent the critical thresholds of biological failure (10). Despite their widespread use, it remains unclear how TPCs and thermal tolerance limits are related and whether the processes governing sublethal performance are fundamentally shared with, or distinct from, those underlying failure at thermal extremes (11). Developing an integrative understanding of biological responses to temperature is critical to characterizing the fundamental ecology of ectotherms and for informing predictions of species performance in the context of global change.

Temperature-dependent performance likely arises from the integration of several distinct mechanistic processes, including kinetic effects on biochemical reaction rates (12, 13), the balance between cellular and molecular damage and repair (7, 14–16), and constraints imposed by oxygen supply and demand (17, 18). Although a unifying framework has yet to be established, the near universality of TPC shape across ectotherms suggests common underlying constraints (12, 13) that may extend to heat tolerance limits (12, 13, 19). In this context, thermal tolerance limits may reflect the functional endpoint where the same processes constraining sublethal performance propagate to whole-organismal failure. Within the damage–repair framework, for instance, performance begins to decline as damage accumulation begins to outpace repair capacity and thermal tolerance limits would represent the point at which cumulative damage effects propagate to organismal failure (13, 19). Similarly, under the oxygen supply/demand framework, performance decreases when metabolic demands outpace the capacity to deliver oxygen (17, 18, 20); thermal tolerance limits may capture the endpoint when transport capacity is fully exhausted, triggering a transition to anaerobic respiration and eventual systemic collapse (21).

Alternatively, thermal tolerance limits may reflect functional endpoints that arise from different processes than sublethal performance. TPCs primarily encompass temperatures where organismal function is maintained, reflecting the balance of metabolism, resource allocation, and damage repair. In contrast, thermal tolerance limits may emerge from the abrupt breakdown of critical physiological systems. At high temperatures, organisms may experience loss of neural function (22), disruption of cardiac electrical excitability (23), destabilization of membrane and ion channel regulation (24), or oxygen limitation (12, 22), with CTmax representing the first system to fail. As a result, thermal tolerance limits may be better characterized by functional

endpoints rather than as the outcome of continuous, rate-dependent processes like those captured in TPCs and may operate on a different timescale than the steady-state dynamics shaping performance (i.e., “stressful range” versus “permissive range”) (13, 19). These differences are potentially reinforced by experimental design: thermal tolerance limits often capture responses to rapid, acute thermal stress, whereas TPCs can be quantified across a range of exposure durations. Longer exposure times can allow plasticity and bioenergetic constraints to influence performance (25), potentially integrating processes that are not captured by the rapid temperature exposure typical of tolerance assays. Consistent with this decoupling, the molecular processes that prepare or maintain function have been found to differ from those that determine failure under acute stress (26). Together, these differences suggest that temperature-dependent performance and thermal tolerance limits may represent partially or wholly independent traits, governed by distinct cellular, molecular, and genetic mechanisms (27, 28), and capable of evolving independently.

Despite their foundational role in thermal biology, the degree to which thermal performance curves and thermal tolerance limits reflect shared underlying constraints across species remains unclear, motivating explicit tests of their covariation among taxa. Here, we synthesize a novel dataset of TPCs and thermal tolerance limits across ectotherms to test the extent to which these thermal traits are related across species. Given the increasing use of thermal traits in assessing ectotherm risk from warming (11), we focus our analyses on TPC traits and thermal tolerance limits that are relevant at high temperatures: the optimal temperature for performance (Topt), the maximum temperature of performance (TPCmax), the supra-optimal range (SOR; the difference between TPCmax and Topt), and critical thermal maximum (CTmax) (Figure 1). If the processes shaping TPCs also govern CTmax, then TPC traits and CTmax should co-vary across species. However, the strength of these relationships may depend on the performance response type used to quantify TPCs, the biological scale at which performance is measured, and the duration of thermal exposure captured (detailed in Table 1). Our null expectation is that TPCs are unrelated to CTmax because they reflect distinct processes. Positive relationships between TPCs and CTmax would indicate that these measures share underlying mechanistic processes, and isometric (1:1) positive relationships would suggest a high degree of conserved overlap between these underlying processes. We therefore evaluate support for relationships between TPCs and CTmax based on their proximity to a 1:1 relationship. By characterizing the shape of the relationship between performance at thermal extremes and permissive temperatures, we advance our understanding of how these thermal traits are related across species.

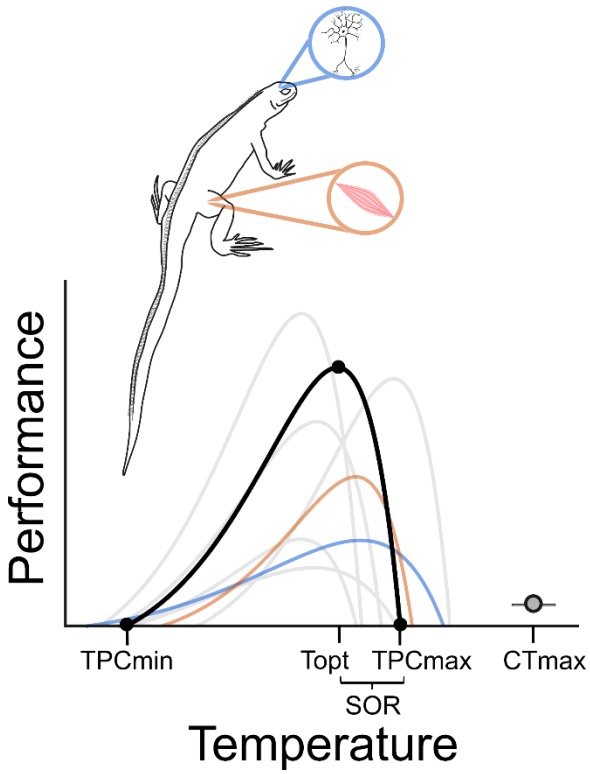

Figure 1. Conceptual illustration of a thermal performance curve (TPC) in black depicting key TPC traits, including the minimum and maximum performance temperature (TPCmin, TPCmax, respectively), the optimal temperature (Topt), and the supra-optimal range (SOR: the range between TPCmax and Topt). The critical thermal maximum (CTmax) is indicated for reference and typically occurs at temperatures exceeding those associated with optimal or maximal performance**.** The aggregation of underlying temperature-dependent processes results in the emerging TPC for a single integrated measure of performance (7). For example, the TPC for running speed (shown in black) reflects the effects of contributing physiological processes (grey), including muscular (orange) and neuronal (blue) performance. TPCs were drawn using hypothetical parameters and the Thomas 2012 model (29) of thermal performance.

Table 1. Descriptions and predicted outcomes for three non-mutually exclusive hypotheses tested here explaining variation in the relationships between thermal performance curve (TPC) traits (Topt and TPCmax) and heat tolerance (CTmax). Here and in the results, we use color to indicate whether the relationship is proportional (blue) or sub-proportional (shades of orange). We interpret proportional (isometric) scaling as the strongest support for the corresponding response being shaped by similar temperature-dependent processes as CTmax.

	Description & Prediction	Prediction Figure
Response Type Hypothesis	The strength and proportionality of TPC-CTmax relationships depend on the degree to which measured TPC responses integrate physiological processes that overlap with those determining CTmax. Because CTmax in animals is often measured as a neuromuscular response (e.g., loss of righting response), we expect that locomotor TPC traits will reflect many of the same integrated physiological processes as CTmax and thus scale near-proportionally with CTmax, while other traits, such as metabolism or life history traits, will demonstrate sub-proportional relationships with CTmax.	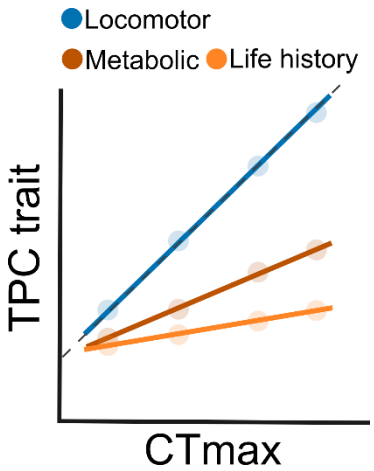
Biological Scale Hypothesis	TPC-CTmax relationships vary across levels of biological organization, reflecting aggregation of processes across biological scales. Because CTmax is measured at the organismal level, we expect proportional scaling between organismal TPCs and CTmax. However, we expect that TPCs measured at other biological scales will show sub-proportional relationships with CTmax, reflecting aggregation that is constrained by biological scale. We expect mean TPC trait values to differ across levels of biological organization, with the highest values for sub-organismal TPCs and the lowest values for population TPCs (30). This is demonstrated as different intercepts in the prediction panel.	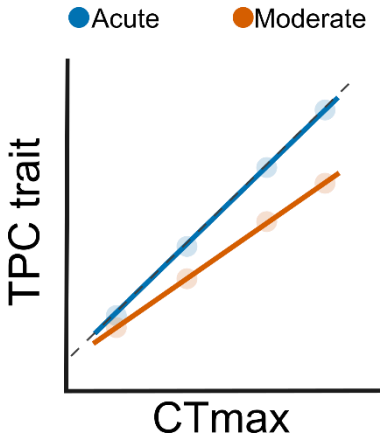

Exposure Duration Hypothesis	We hypothesize that the experimental timescale of TPC measurement influences its relationship with CTmax. Because CTmax represents an acute thermal endpoint, we predict that acutely measured TPCs will exhibit closer-to-proportional relationships, whereas TPCs measured over longer (moderate) timescales will scale sub-proportionally with CTmax.	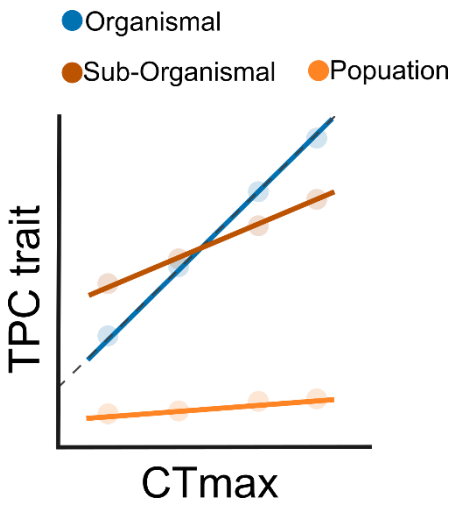

154

Methods

To test our hypotheses about the relationships between thermal performance curves (TPC) and maximum temperature tolerance (CTmax), we assembled a dataset of TPCs (N = 1584 species) and CTmax (N = 2703 species) from terrestrial, marine, and freshwater systems. We identified 197 species with both TPC and CTmax data and used non-linear models to fit TPCs to the performance values. From each curve, we derived the temperature of peak performance (thermal optimum, Topt), the maximum temperature of positive performance (TPCmax), and the supra-optimal range (SOR; the range of temperatures between Topt and TPCmax). We used a hierarchical mixed effects modeling approach to test for the strength and proportionality of relationships between each TPC trait and CTmax. Finally, we used a model comparison approach to identify the set of predictors that best explained variation in TPC traits.

Sources of data

Our dataset integrates (i) thermal performance data (to which we fitted TPCs and quantified Topt, TPCmax and SOR), (ii) maximum thermal tolerance limits (CTmax), and (iii) plasticity in CTmax for ectotherms across major taxa.

Thermal performance data: We compiled data to fit TPCs through a broad literature search (Web of Science, Google Scholar) and targeted searches for species with known CTmax. We retained studies that experimentally manipulated temperature and reported performance values across ≥5 temperature treatments. We extracted performance values and metadata from text, tables, or digitized figures using WebPlotDigitizer v5.2 (31) and standardized them to common units (e.g., durations were converted to rates). We combined the results of our TPC searches (N=428) with data from published datasets of ectotherm thermal performance estimates ((32) N = 2739; (33) N = 194).

To support our hypothesis testing, we classified performance values by response type (metabolic, locomotion, life history) and level of biological organization (sub-organismal, organismal, population). We also classified performance assays by duration to capture the potential for plasticity and bioenergetic constraints to influence performance during the experiment. Assays lasting ≥ 30 minutes –long enough for physiological responses such as the upregulation of heat-shock proteins (e.g.,(34))– were classified as “moderate” in duration, while assays < 30 minutes were classified as “acute”.

Upper thermal tolerance limits: We compiled CTmax values from existing ectotherm thermal-limit databases ((35) N = 485; (36) N = 587; (37) N = 1590, (38) N = 689) and targeted species-specific searches of species with thermal performance data (resulting in an additional N = 19). We retained all measurements of upper thermal limits (e.g., maximum temperature at which the onset of muscle spasms occurs, the temperature at which organisms no longer right themselves, lethal dose 50% mortality) and refer to them collectively as CTmax. For each record, we

recorded acclimation temperature or recovered it from original sources, including field temperatures when relevant.

Plasticity in CTmax: To account for the effects of acclimation temperature on CTmax (39–41), we compiled data on acclimation response ratios (ARR), which measures the magnitude of change in CTmax per degree increase in acclimation/holding temperature (*SI Appendix* - Equation S1). We compiled species-specific CTmax ARRs from ((36) N = 179) ((42) N = 320) ((43) N = 95) ((44) N = 21) ((45) N = 24). For studies reporting CTmax estimates from multiple acclimation temperatures, we calculated ARR using estimates from the minimum and maximum acclimation temperatures.

We standardized CTmax values to a common acclimation temperature (*SI Appendix* - Equation S2) using taxon-summarised ARRs. Because CTmax values standardized using ARR means from different taxonomic levels were highly correlated with one another and with unstandardized CTmax (Table S1), we used phylum-level mean ARRs for all subsequent analyses. Results are presented using CTmax standardized to 15°C, the mean global surface temperature (NOAA 2024 Annual eport), although our conclusions were robust to the choice of standardization temperature (Figure S1).

Further details on search protocols, data extraction and metadata classifications, and ARR standardization are provided in the *SI Appendix* - Data Sources.

TPC Fitting and Quality Control

We fit thermal performance curves (TPCs) using non-linear least squares (nlsLM, *minpack.lm* in R) and the Norberg model (46) as modified by (29) (referred to as the Norberg-Thomas model) (Equation 1). We chose the Norberg-Thomas model because it accommodates both left- and right-skewed curves, requires only four parameters, and is suitable for datasets with ≥ 5 temperature points. In the Norberg-Thomas model, *a* acts as a scaling parameter, *b* determines the slope of the exponential rise and the direction of the curve skew, *c* captures the breadth of positive performance, and *Tref* is the temperature at which the decay function peaks.

$$f(T) = a \cdot e^{bT}\left[1 - \left(\frac{T - Tref}{(\frac{c}{2})}\right)^2\right]$$

Equation 1

Curve fitting proceeded in up to three rounds, with quality control applied after each (see SI Appendix - TPC Fitting and Quality Control for more details). Because curves yielding high confidence in Topt estimates were not always the same as those with high confidence in TPCmax, quality control was performed independently for each trait to maximize the number of

curves retained. Initial fits used data-informed starting values and broad parameter bounds. To quantify uncertainty, we generated 10,000 non-parametric bootstrap curves per TPC. We calculated Topt and TPCmax from parameter sets for each bootstrap: we calculated TPCmax as $Tref + c/2$ (Equation 1); we calculated Topt via numerical optimization. We excluded curves with imprecise trait estimates (95% CI >15% of c in Equation 1) or parameter estimates near the bounds. Curves failing these criteria were refit using multiple randomized starts, and if still unsuccessful, refit with constrained skew parameter starting values. For curves passing this filtering step, we identified the 95% confidence interval of each TPC trait estimate (e.g., Topt) and retained 1,000 randomly sampled bootstrap parameter sets whose associated trait values fell within this interval. As a final filter, we excluded TPCs with high trait uncertainty (CI > 5 °C). Therefore, TPC fitting and quality control resulted in two datasets—one optimized for Topt and one for TPCmax—each retaining 1,000 randomly sampled bootstrap parameter sets that passed all quality-control filters.

Statistical Analyses

Across all sources, we compiled 2,069 TPCs for 850 species, 8077 CTmax estimates for 2932 species, and 678 ARR estimates for 475 species. After model fitting and quality control, we retained 204 TPCs (102 species) with Topt estimates, and 159 TPCs (79 species) with TPCmax estimates (Figure S2). From these, 153 TPCs (75 species) contained had both Topt and TPCmax estimates, which were used to calculate the supra-optimal range of performance (SOR) and to compare relative variation among thermal traits.

We conducted all analyses in R v4.5.1. We tested for relationships between TPC traits (TPCmax, Topt, SOR) and CTmax using multilevel meta-regressions fitted using restricted maximum likelihood. This regression approach incorporates known sampling variances, accommodates unbalanced data, and allows flexible random-effects structures. For each TPC trait model, we used the mean of 1,000 bootstrap estimates as the response and their variance as weights (*rma.mv*, *metafor*,(47)). We accounted for phylogenetic non-independence among TPCs by including a taxonomic classification as a random intercept in these models. We compared models with different taxonomic classification as a random intercept via Akaike Information Criterion (AIC, (48)) and selected Class as the most appropriate structure for subsequent models (Table S2). As an initial step, we tested for overall relationships between each TPC trait and CTmax. In all models, CTmax was standardized (z-scored) by subtracting the dataset mean and dividing by the SD, allowing comparison of effect sizes across models. For the Topt models, CTmax was scaled to a mean of 37.42 °C (SD = 9.17); for TPCmax models, CTmax was scaled to a mean of 38.12 °C (SD = 9.69). These models established the direction, strength, and scaling of TPC–CTmax relationships in the absence of additional predictors and provided a reference for subsequent hypothesis-driven analyses. For interpretability, figures are presented in the main text on the original temperature scale and in the *SI Appendix* on the scaled axis.

We then evaluated support for hypotheses predicting variation in TPC–CTmax relationships across response type, biological scale, and exposure duration. For each hypothesized predictor, we fitted meta-regression models with the hypothesized predictor as a fixed effect, both independently and in interaction with CTmax. Because many categorical predictors were non-exclusive and some predictor combinations were unevenly represented (Figure S3), we first evaluated support for each hypothesis using separate, independent models. All models included Class as a random intercept. To identify which predictors across all hypotheses best explained the TPC data, we used the results from the hypothesis-specific models to guide construction of a global model (to avoid overparameterization) and compared this global model to all subsets using AIC. Finally, we tested the relationship between the supra-optimal range (SOR) and CTmax using an additional multilevel regression fitted with restricted maximum likelihood. We treated SOR as the response variable (with its sampling variance propagated from uncertainty in Topt and TPCmax and included as known variances), CTmax as the predictor, and Class as a random intercept.

We assessed model support by comparison to an intercept-only model containing Class as a random intercept via AIC and pseudo-R^2 (reduction in among-Class variance relative to the intercept-only model) and using moderator tests (QM). We evaluated support for individual predictors using Wald-type tests of whether coefficients differed from zero and 95% confidence intervals. We interpreted the strength and direction of predictor-CTmax relationships (i.e., the interaction term of the model) and whether slopes and CIs overlapped the isometric (proportional) expectation.

Results

TPC traits were positively related to CTmax across ectotherms.

We found strong positive relationships between TPC traits (Topt, TPCmax) and maximum heat tolerance (CTmax) when accounting for among-Class variance in our multi-level mixed-effects models (Figure 2). Models linking Topt to CTmax (N=204 and TPCmax to CTmax (N=159) both fit the data better (AIC), explained substantially more among-Class variance than their respective intercept-only (null) models (*pseudo*-R^2), and contained significant predictors (QM test) (all metrics reported in Table S3). The slope of the relationship between TPCmax and CTmax was greater than that of Topt and CTmax (Topt: slope = 6.34, 95% CI [6.27, 6.41], $p < 0.001$, *pseudo*-$R^2 = 0.12$); TPCmax: slope = 7.87, 95% CI [7.77, 7.97], $p < 0.001$, *pseudo*-$R^2 = 0.62$), though both relationships had shallower slopes than isometry. Across all hypothesis-specific models presented below, TPC traits were positively related to CTmax.

Species with higher CTmax also exhibited broader supra-optimal ranges (SOR) (Figure 2). A multi-level mixed effects model (N = 153 TPCs, 75 species) accounting for Class as a random intercept estimated a positive, sub-proportional relationship between SOR and CTmax (slope = 0.55 [0.54, 0.56], $p < 0.001$, *pseudo*-$R^2 = 0.28$, Table S4).

The magnitude of absolute variation was remarkedly consistent across the upper thermal niche (Figure 2). Bootstrapped mean standard deviation and 95% confidence intervals (CIs) revealed nearly identical levels of variation for TPCmax (sd = 9.48 [8.63, 10.3]) and CTmax (sd = 9.75 [8.66, 10.8]), suggesting shared evolutionary constraints between these traits. While Topt demonstrated slightly lower absolute variation (sd = 8.24 [7.47, 9.08]), the values remained similar in magnitude. Absolute variation was lowest for SOR (sd = 4.84 [4.16, 5.53]), although this was expected as SOR represents a derived product of covariation in TPCmax and Topt rather than an independent trait.

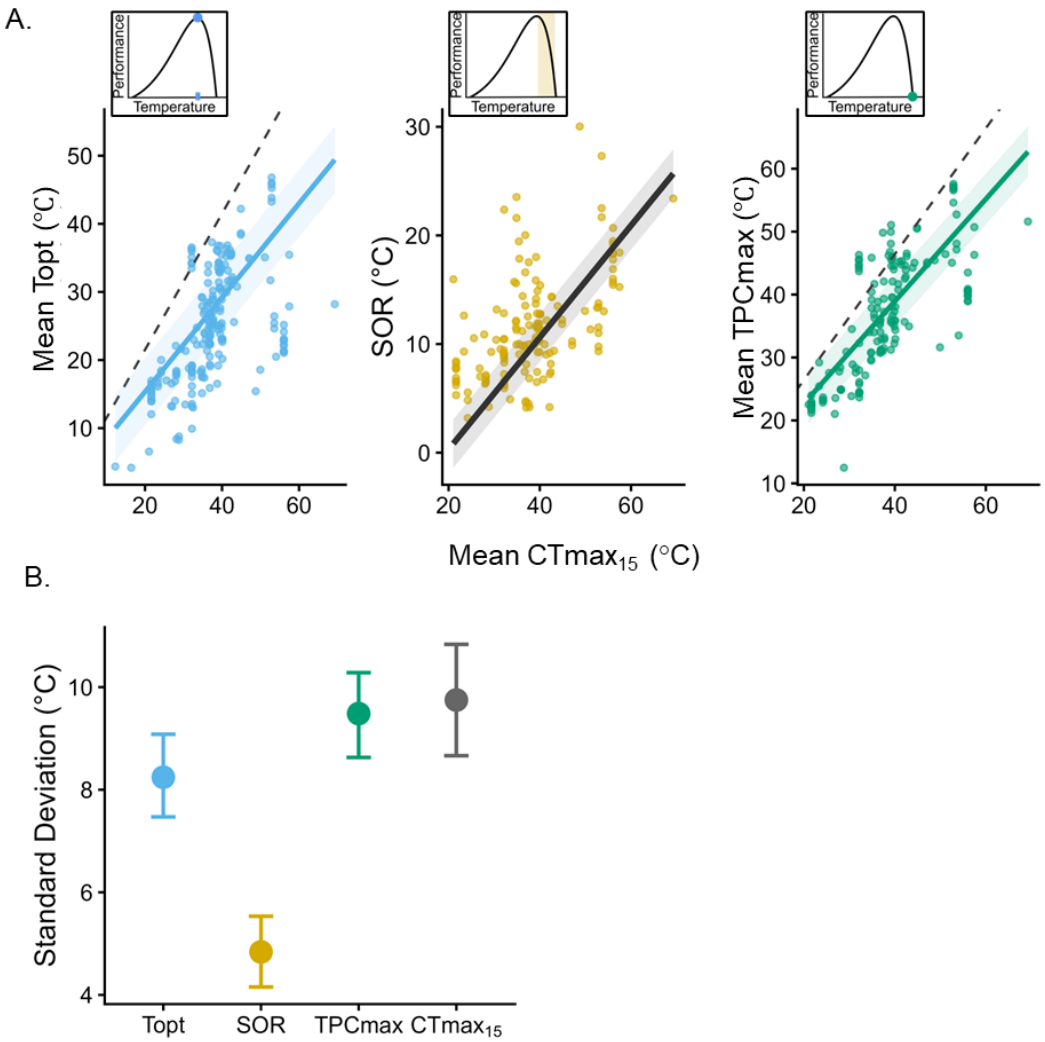

Figure 2. A: Topt (blue; N = 204, 102 species), the supra-optimal range (SOR; yellow; N = 153 TPCs, 75 species), and TPCmax (green; N = 159, 79 species) increased with CTmax. Points represent the mean of 1,000 bootstrapped estimates from each fitted thermal performance curve; for SOR, points represent TPC-level values calculated as the difference between TPCmax and Topt. Species mean CTmax values were ARR-standardized to an acclimation temperature of 15°C (Eq. S2) and scaled for model fitting (Topt mean = 37.42, SD = 9.17; TPCmax mean = 38.12, SD = 9.69); model projections are back-transformed to the original temperature scale for interpretability. Solid lines show model-predicted relationships with shaded ribbons indicating 95% confidence intervals. The grey dashed line indicates the proportionality expectation. **B:** Points and bars represent the mean standard deviation and 95% confidence interval of 1,000 bootstrapped estimates for each thermal trait.

Response type hypothesis – We found support for our hypothesis that TPC-CTmax relationships depend on the type of biological response measured by TPCs (Figure 3A). This dependence was characterized by using a multi-level regression model fitted to TPC trait data testing for an interaction between CTmax and biological response category (locomotion or metabolic). We excluded plants (which lacked locomotion data, N=26) and life history traits (due to small sample size, N = 5), resulting in datasets focused on animal ectotherms (Topt: $N_{\text{metabolic processes}}$ = 64, $N_{\text{locomotion}}$ = 107; TPCmax: $N_{\text{metabolic processes}}$ = 53, $N_{\text{locomotion}}$ = 75). Both the Topt and TPCmax models revealed that locomotion TPCs exhibited significantly stronger relationships with CTmax than metabolic TPCs (Topt: locomotion slope = 8.91 [8.61, 9.22], metabolic slope = 5.43 [5.31, 5.55], $p_{\text{interaction}} < 0.001$, *pseudo*-$R^2$ = 0.02; TPCmax: locomotion slope = 9.16 [8.82, 9.49], metabolic slope = 5.77 [5.64, 5.90], $p_{\text{interaction}} < 0.001$, *pseudo*-$R^2$ = 0.32; Table S5). Notably, the slope of the relationship between locomotion Topt and CTmax overlapped the isometric expectation (9.17), indicating that increases in CTmax were accompanied by proportional increases in thermal optima for locomotor processes. While the relationship between locomotion TPCmax and CTmax was slightly less than proportional, it was the closest to proportionality among all predictors tested.

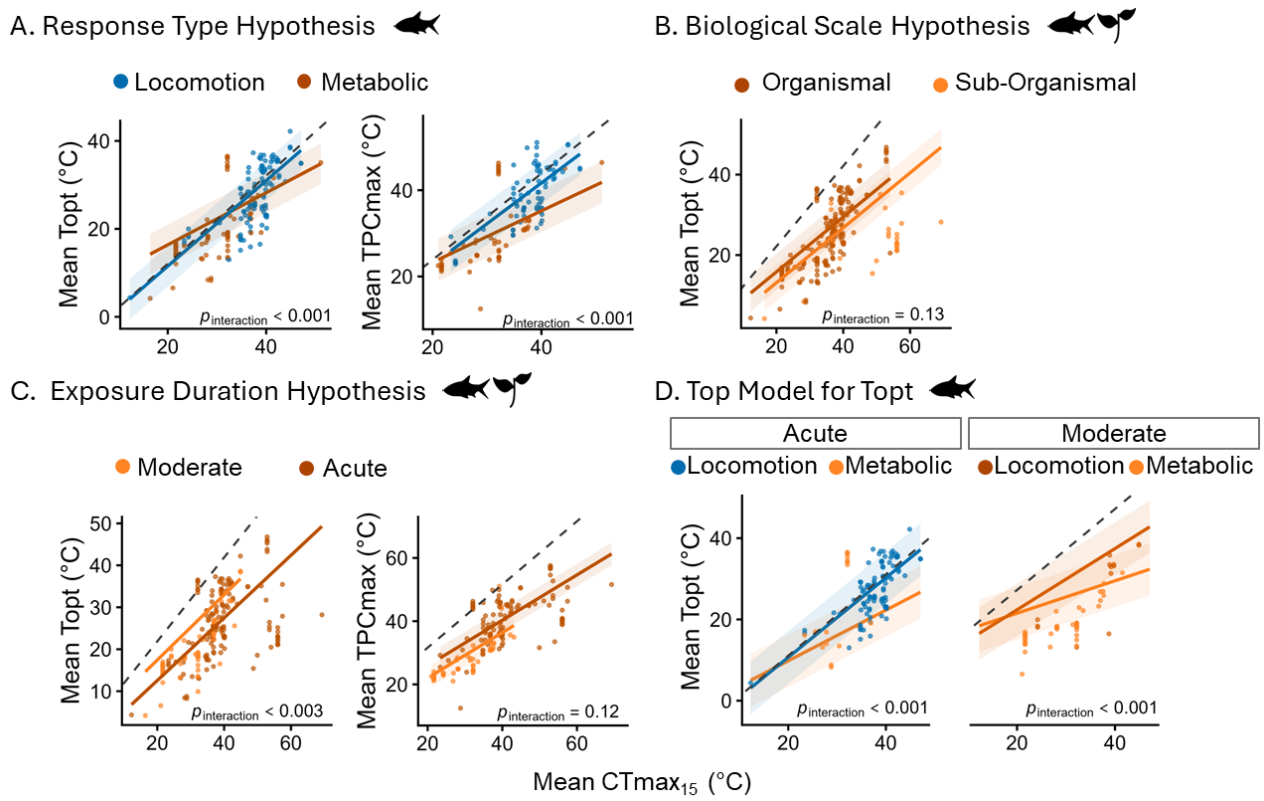

Figure 3. Relationships between thermal performance curve (TPC) traits and CTmax from our single hypothesis models (A-C) and the top model for Topt following a model selection approach (D). Model projections are back-transformed to the original temperature scale. Panels show (A) Response type hypothesis (N_{Topt} = 171; N_{TPCmax} = 111), (B) Biological scale hypothesis (N_{Topt} = 202), (C) Exposure duration hypothesis (N_{Topt} = 204, N_{TPCmax} = 159), and (D) the top-ranked model for Topt (N = 162), which includes exposure duration and response type as predictors. For all panels, points represent mean TPC trait estimates derived from 1,000 bootstrap fits, solid lines indicate model-predicted relationships, and shaded ribbons show 95% confidence intervals. $CTmax_{15}$ refers to species mean CTmax when standardized to an acclimation temperature of 15°C using phylum-averaged acclimation response ratios. Note that the prediction lines do not account for random Class effects. Grey dashed lines denote proportionality expectations with the intercept set to the highest group intercept. Blue lines indicate that the corresponding slope overlaps with the expectation of proportionality while orange lines (both dark orange and light orange) denote sub-proportionality. The fish icon denotes the model includes animals; the plant icon denotes the model includes plants.

Biological scale hypothesis – We did not find support for our hypothesis that TPC-CTmax relationships depend on the level of biological organization at which TPCs are measured. Multi-level regression models to fitted Topt data ($N_{organismal}$ = 174, $N_{suborganismal}$ = 28, excluding N = 2 population-level TPCs) exhibited a non-significant interaction term (Table S6), indicating that Topt from sub-organismal and organismal TPCs demonstrated the same sub-isometric relationship with CTmax (slope coefficient 6.26 [6.19, 6.33], $p < 0.001$, *pseudo*-R^2 = 0.26) (Figure 3B). While the slopes were the same, Topt values were generally lower from the sub-organismal level than from the organismal level (sub-organismal intercept in reference to organismal intercept -2.69 [-2.93, -2.44], $p < 0.001$). Note that we were unable to robustly test for biological scale effects on the TPCmax–CTmax relationship due to sample size imbalances ($N_{population}$ = 2, $N_{organismal}$ = 136, $N_{suborganismal}$ = 21) and an over-representation of plant species in the sub-organismal category (19 of 21), which would bias estimates of among-Class variance.

Exposure duration hypothesis – We found mixed support for the hypothesis that TPC-CTmax relationships vary with TPC assay duration (Figure 3C). Multi-level regression models indicated sub-proportional scaling with CTmax across both acute and moderate duration TPCs (Topt: N_{acute} = 141, $N_{moderate}$ = 63; TPCmax N_{acute} = 108, $N_{moderate}$ = 51). Specifically, Topt slopes were 6.84 [6.69, 6.98] for acute and 7.13 [6.83, 7.43] for moderate exposures ($p_{interaction}$ = 0.002, *pseudo*-R^2 = 0.03). For TPCmax, acute and moderate slopes did not statistically differ (acute slope = 6.84 [6.67, 7.01], moderate slope = 7.00 [6.63 7.37], $p_{interaction}$ = 0.12, *pseudo*-R^2 = 0.71; Table S7). Contrary to our prediction that acute-exposure slopes would be closer to isometric expectations, slopes were closer to isometry when TPCs reflected longer temperature exposure assays ('moderate' duration). However, although the interaction term for the Topt-CTmax model was statistically significant, the substantial overlap in 95% confidence intervals suggest that the functional differences between these categories are minimal. Overall, these relationships indicate that TPC-CTmax relationships are consistently sub-proportional and largely similar across assay durations tested here.

Topt for acute locomotion processes increased proportionally with CTmax across animal ectotherms.

We used a model-comparison approach to identify the predictors that best explained variation between CTmax and Topt. Based on hypothesis-specific support, we constructed a global model including trait response type and exposure duration as both main effects and in interaction with CTmax. Because biological scale showed little support for modifying TPC–CTmax relationships and caused severe data imbalances, we restricted this analysis to organismal-level TPCs (N = 162 TPCs, 85 species). Additionally, because plants were not represented in locomotion TPCs, they were excluded to allow direct comparison of physiological processes. Data limitations precluded a similar approach for TPCmax due to sample size imbalances that prevented reliable estimation of interaction effects.

The fully parameterized model was retained as the sole top model for Topt (ΔAICc < 2; Table S8) and was a substantially better fit than the intercept-only null model (ΔAIC = 44630.75). While the high level of residual heterogeneity (SD ≈ 8.7) resulted in a negligible *pseudo*-R^2, the large improvement in AIC and the significant Test of Moderators (QM = 44,642.9, $p < 0.001$) demonstrate that the included fixed effects are critical for explaining the observed variation in Topt. Results indicated that Topt for acute locomotion scaled proportionally with CTmax across species (slope=8.97 [8.76, 9.19], p < 0.001; Table S9), whereas Topt for moderate-duration locomotion traits increased sub-proportionally with CTmax (slope = 6.93 [6.75, 7.11], p < 0.001). In contrast, Topt for metabolic traits scaled sub-proportionally with CTmax regardless of assay duration ($slope_{acute}$ = 5.72 [5.45, 5.99], $slope_{moderate}$ = 3.68 [3.55, 3.80], p < 0.001). Consistent with our initial predictions, slopes for moderate-duration assays were lower than those for acute assays in this integrated model (Figure 3D). The apparent reversal of duration effects compared to the independent hypothesis model is likely attributable to the exclusion of plants or variation interacting with response types. Indeed, when the single-hypothesis model for exposure duration was restricted to animals, Topt from moderate-duration assays increased with CTmax at a lower rate than Topt from acute TPC assays (Table S10).

Discussion

Our analysis of over 100 ectotherm species reveals that maximum heat tolerance (CTmax) is not an independent threshold of acute failure at high temperature extremes but rather is fundamentally coupled with performance at sublethal temperatures. We found that species with higher CTmax consistently exhibited higher thermal optima (Topt) and thermal maxima (TPCmax), as well as a wider supra-optimal range of performance (SOR). These results provide empirical support for the hypothesis that the mechanistic processes governing temperature-dependent performance, such as biochemical reaction rates and the balance of cellular damage and repair, are related to the processes that ultimately propagate to organismal failure at extreme temperatures (13, 19). By demonstrating that CTmax contains meaningful information about variation in TPCs, including the breadth of performance decline (SOR), our results suggest that heat tolerance and temperature-dependent performance may be governed by shared, rather than decoupled, physiological processes.

While broad positive relationships suggest shared mechanisms, the form of the relationship provides insight into the strength of coupling between TPCs and CTmax. Our results suggest that the strength of coupling is driven by both the type of biological response being measured and the timescale of the assay. Specifically, proportional (1:1) scaling was restricted to acute locomotor responses, suggesting that the locomotor system is fundamentally related to tolerance limits captured by CTmax. Because CTmax assays for animals define failure as the loss of coordinated movement, CTmax may reflect the terminal endpoint of the same mechanistic processes governing locomotor Topt. As the timescale of the locomotor assay increased to moderate durations, this relationship became sub-proportional. This shift suggests that while the underlying neuromuscular mechanisms may remain consistent, time-dependent constraints— such as bioenergetic depletion and plasticity (15)— may begin to decouple Topt from organismal failure.

Unlike the proportional scaling observed for acute locomotor traits, metabolic responses consistently exhibited sub-proportional relationships with CTmax. Consequently, in heat tolerant species, sub-proportional relationships led to a widening gap between metabolic thermal optima and absolute thermal tolerance. This divergence suggests that metabolic responses (e.g., somatic growth rate, consumption rate, respiration rate) are driven by partially independent processes than the ones captured by CTmax. While locomotion may be related to CTmax through a strong overlap in mechanistic similarity, metabolic performance may reflect a broader array of cellular and systemic functions that reach their limits at different endpoints. Furthermore, these divergent scaling patterns may reflect difference in the selective landscape for these traits. While the processes underlying performance and failure in locomotion may be under similar selection pressures, metabolic responses may be subject to different multivariate selection pressures due to their involvement in many aspects of organismal growth, maintenance, and reproduction.

Given that Topt and TPCmax capture different aspects of thermal performance and ecological contexts (6, 49–51), the consistency of their relationships with CTmax is striking. Prior macro-physiological evidence suggests that heat tolerance limits like CTmax are more evolutionarily constrained than cold tolerance limits across species (52–55), leading to the expectation that performance traits capturing non-maximal heat tolerance (e.g., Topt and to a lesser extent TPCmax) should exhibit more variation than CTmax. While we found slightly lower variation in Topt compared to CTmax and TPCmax, the magnitudes of variation were remarkably similar across these traits. The similarity in trait standard deviations—which reflect the history of past selection and the capacity for future evolution— and the correlations we found among TPCs and CTmax suggest that temperature-dependent performance and tolerance may reflect an integrated evolutionary module. Whether this is the outcome of a fundamental mechanistic constraint or correlational selection across the thermal niche remains to be tested. Nonetheless, a similar magnitude of variation does not imply a similar biological consequence. Due to the non-linear, asymmetric shape of the TPC (Figure 1)(56), small shifts in relative performance at the warm-end of the curve and upper tolerance limits can have disproportionate impacts on fitness relative to equivalent shifts in Topt (57, 58). For example, minor increases in CTmax have been shown to significantly decrease the probability of mortality during heating events (59). Conversely, in environments where temperatures rarely approach CTmax, selection may act more strongly on temperatures that maximize daily performance, such as Topt and SOR. Thus, while CTmax, Topt, and TPCmax may exhibit similar amounts of variation, the relative fitness value of that variation is dependent on the frequency and intensity of thermal stress in the environment.

The patterns uncovered here help reconcile a long-standing debate about the utility of CTmax in studies of relative vulnerability to warming temperatures (11, 60). Although CTmax captures failure endpoints that may rarely be experienced in nature (54, 61), its strong positive relationships with TPC traits provide an empirical link to thermal traits relevant to temperatures frequently experienced in nature and directly tied to fitness. This link is particularly evident within the supra-optimal range (SOR), the temperatures capturing declining performance before failure. We found that species with higher CTmax had wider SORs, suggesting that the processes enabling performance at high temperatures may be related to those underlying absolute tolerance. Consequently, in the absence of TPCs, CTmax may provide a practical, *comparative* metric for identifying species capable of maintaining functional performance across a range of warm temperatures, even if fitness begins to decline before CTmax is reached. However, the consistently sub-proportional relationship with metabolic responses suggests that vulnerability insights from CTmax may overestimate safety margins for processes such as growth and maintenance. While the relative ease of experimentally estimating CTmax, and its widespread availability in the literature makes it an indispensable first step in large-scale assessments of thermal risk across many taxa, accurately forecasting population persistence still requires TPCs to capture the non-linear cumulative performance impact of temperature over broad temperature ranges.

Ultimately, our results provide an empirical basis for incorporating organismal physiology into population-level forecasting models (15, 16, 62–64). We show that while CTmax and TPCs are strongly related, the relationships among them are frequently non-proportional, a critical distinction for predicting responses to both extreme heatwaves and chronic, sub-lethal thermal stress (16). While CTmax captures meaningful variation in acute locomotor performance, its sub-proportional scaling with metabolic traits underlying growth suggests that relying solely on tolerance limits risks missing other effects of temperature causing organisms and populations fail. Moving forward, resolving the phylogenetic structure of these relationships, and their genetic and plastic bases, will be critical for refining our understanding of how thermal traits vary across ectotherms. By providing an explicitly multivariate understanding of temperature-dependent traits, we connect our understanding of the processes that maintain performance over temperatures with those that cause organismal performance to fail, improving our ability to project species persistence in a warming world.

References

1. G. N. Somero, Adaptation of enzymes to temperature: Searching for basic "strategies." *Comparative Biochemistry and Physiology - B Biochemistry and Molecular Biology* **139**, 321–333 (2004).

2. P. W. Hochachka, G. N. Somero, *Biochemical Adaptation: Mechanism and Process in Physiological Evolution* (Oxford University Press, 2002).

3. M. J. Angilletta, *Thermal Adaptation: A Theoretical and Empirical Synthesis* (Oxford University Press, 2009).

4. P. Amarasekare, V. Savage, A framework for elucidating the temperature dependence of fitness. *Am. Nat.* **179**, 178–191 (2012).

5. R. B. Huey, J. G. Kingsolver, Evolution of thermal sensitivity of ectotherm performance. *Trends Ecol. Evol.* **4**, 131–135 (1989).

6. B. L. Bodensteiner, *et al.*, Thermal adaptation revisited: How conserved are thermal traits of reptiles and amphibians? *Journal of Experimental Zoology Part A: Ecological and Integrative Physiology* **335**, 173–194 (2021).

7. L. B. Buckley, R. B. Huey, C.-S. Ma, How damage, recovery, and repair alter the fitness impacts of thermal stress. *Integr. Comp. Biol.* **65**, 1061–1075 (2025).

8. F. Bozinovic, *et al.*, Thermal effects vary predictably across levels of organization: empirical results and theoretical basis. *Proc. Biol. Sci.* **287**, 20202508 (2020).

9. P. M. Schulte, The effects of temperature on aerobic metabolism: towards a mechanistic understanding of the responses of ectotherms to a changing environment. *J. Exp. Biol.* **218**, 1856–1866 (2015).

10. R. B. Cowles, C. M. Bogert, A preliminary study of the thermal requirements of desert reptiles. *Bull. Am. Mus. Nat. Hist.* **83** (1944).

11. S. Clusella-Trullas, R. A. Garcia, J. S. Terblanche, A. A. Hoffmann, How useful are thermal vulnerability indices? *Trends Ecol. Evol.* **36**, 1000–1010 (2021).

12. R. Ern, A. H. Andreassen, F. Jutfelt, Physiological mechanisms of acute upper thermal tolerance in fish. *Physiology (Bethesda)* **38**, 141–158 (2023).

13. M. Ørsted, L. B. Jørgensen, J. Overgaard, Finding the right thermal limit: a framework to reconcile ecological, physiological and methodological aspects of CTmax in ectotherms. *J. Exp. Biol.* **225** (2022).

14. D. González-Tokman, *et al.*, Insect responses to heat: physiological mechanisms, evolution and ecological implications in a warming world. *Biol. Rev. Camb. Philos. Soc.* **95**, 802–821 (2020).

15. J. G. Kingsolver, H. A. Woods, Beyond thermal performance curves: Modeling time-dependent effects of thermal stress on ectotherm growth rates. *Am. Nat.* **187**, 283–294 (2016).

16. P. A. Arnold, *et al.*, A framework for modelling thermal load sensitivity across life. *Glob. Chang. Biol.* **31**, e70315 (2025).

17. H. O. Pörtner, Oxygen- And capacity-limitation of thermal tolerance: A matrix for integrating climate-related stressor effects in marine ecosystems. *J. Exp. Biol.* **213**, 881–893 (2010).

18. H. O. Pörtner, Physiological basis of temperature-dependent biogeography: Trade-offs in muscle design and performance in polar ectotherms. *J. Exp. Biol.* **205**, 2217–2230 (2002).

19. L. B. Jørgensen, H. Malte, M. Ørsted, N. A. Klahn, J. Overgaard, A unifying model to estimate thermal tolerance limits in ectotherms across static, dynamic and fluctuating exposures to thermal stress. *Sci. Rep.* **11**, 12840 (2021).

20. A. P. Farrell, Aerobic scope and its optimum temperature: clarifying their usefulness and limitations - correspondence on J. Exp. Biol. 216, 2771-2782. *J. Exp. Biol.* **216**, 4493–4494 (2013).

21. H. O. Pörtner, R. Knust, Climate change affects marine fishes through the oxygen limitation of thermal tolerance. *Science* **315**, 95–97 (2007).

22. A. H. Andreassen, P. Hall, P. Khatibzadeh, F. Jutfelt, F. Kermen, Brain dysfunction during warming is linked to oxygen limitation in larval zebrafish. *Proc. Natl. Acad. Sci. U. S. A.* **119**, e2207052119 (2022).

23. M. Vornanen, The temperature dependence of electrical excitability in fish hearts. *J. Exp. Biol.* **219**, 1941–1952 (2016).

24. K. Bowler, Heat death in poikilotherms: Is there a common cause? *J. Therm. Biol.* **76**, 77–79 (2018).

25. P. M. Schulte, T. M. Healy, N. A. Fangue, Thermal performance curves, phenotypic plasticity, and the time scales of temperature exposure. *Integr. Comp. Biol.* **51**, 691–702 (2011).

26. M. C. Lecheta, *et al.*, Integrating GWAS and transcriptomics to identify the molecular underpinnings of thermal stress responses in Drosophila melanogaster. *Front. Genet.* **11**, 658 (2020).

27. A. A. Mauro, C. Ghalambor, Trade-offs, pleiotropy, and shared molecular pathways: A unified view of constraints on adaptation. *Integr. Comp. Biol.* (2020). https://doi.org/10.1093/icb/icaa056.

28. A. G. Little, F. Seebacher, Physiological performance curves: When are they useful? *Front. Physiol.* **12**, 805102 (2021).

29. M. K. Thomas, C. T. Kremer, C. A. Klausmeier, E. Litchman, A global pattern of thermal adaptation in marine phytoplankton. *Science* **338**, 1085–1088 (2012).

30. E. Rezende, F. Bozinovic, Thermal performance across levels of biological organization. *Philosophical Transactions - Royal Society of London, B* **374** (2019).

31. A. Rohatgi, *WebPlotDigitizer*.

32. D.-G. Kontopoulos, *et al.*, No universal mathematical model for thermal performance curves across traits and taxonomic groups. *Nat. Commun.* **15**, 8855 (2024).

33. S. Pawar, *et al.*, Variation in temperature of peak trait performance constrains adaptation of arthropod populations to climatic warming. *Nat. Ecol. Evol.* **8**, 500–510 (2024).

34. L. A. Hoekstra, K. L. Montooth, Inducing extra copies of the Hsp70 gene in Drosophila melanogaster increases energetic demand. *BMC Evol. Biol.* **13** (2013).

35. L. Comte, J. D. Olden, Climatic vulnerability of the world's freshwater and marine fishes. *Nat. Clim. Chang.* **7**, 718–722 (2017).

36. P. Pottier, *et al.*, Developmental plasticity in thermal tolerance: Ontogenetic variation, persistence, and future directions. *Ecol. Lett.* **25**, 2245–2268 (2022).

37. J. M. Bennett, *et al.*, GlobTherm, a global database on thermal tolerances for aquatic and terrestrial organisms. *Scientific Data* **5**, 1–7 (2018).

38. L. T. Lancaster, A. M. Humphreys, Global variation in the thermal tolerances of plants. *Proc. Natl. Acad. Sci. U. S. A.* **117**, 13580–13587 (2020).

39. J. H. Stillman, Acclimation capacity underlies susceptibility to climate change. *Science* **301**, 65 (2003).

40. L. S. Peck, S. A. Morley, J. Richard, M. S. Clark, Acclimation and thermal tolerance in Antarctic marine ectotherms. *J. Exp. Biol.* **217**, 16–22 (2014).

41. F. Seebacher, C. R. White, C. E. Franklin, Physiological plasticity increases resilience of ectothermic animals to climate change. *Nat. Clim. Chang.* **5**, 61–66 (2015).

42. S. A. Morley, L. S. Peck, J. M. Sunday, S. Heiser, A. E. Bates, Physiological acclimation and persistence of ectothermic species under extreme heat events. *Glob. Ecol. Biogeogr.* **28**, 1018–1037 (2019).

43. A. R. Gunderson, M. E. Dillon, J. H. Stillman, Estimating the benefits of plasticity in ectotherm heat tolerance under natural thermal variability. *Funct. Ecol.* **31**, 1529–1539 (2017).

44. L. Zhu, *et al.*, Plasticity of photosynthetic heat tolerance in plants adapted to thermally contrasting biomes. *Plant Cell Environ.* **41**, 1251–1262 (2018).

45. R. J. Harris, *et al.*, Acclimation of thermal tolerance in juvenile plants from three biomes is suppressed when extremes co-occur. *Conserv. Physiol.* **12**, coae027 (2024).

46. J. Norberg, Biodiversity and ecosystem functioning: A complex adaptive systems approach. *Limnol. Oceanogr.* **49**, 1269–1277 (2004).

47. W. Viechtbauer, Conducting Meta-Analyses in R with the metafor Package. *J. Stat. Softw.* **36**, 1–48 (2010).

48. H. Akaike, Information Theory and an Extension of the Maximum Likelihood Principle in *Proceedings of the 2nd International Symposium on Information Theory*, B. N. Petrov, F. Csaki, Eds. (1973), pp. 267–281.

49. R. B. Huey, "Temperature, physiology, and the ecology of reptiles" in *Biology of the Reptilia*, F. H. P. C. Gans, Ed. (Academic Press, 1982), pp. 25–91.

50. Huey, R. B. & Kingsolver, J G, Evolution of Resistance to High Temperature in Ectotherms. *Am. Nat.* **142**, 21–46 (1993).

51. M. J. Angilletta Jr, *et al.*, Coadaptation: a unifying principle in evolutionary thermal biology. *Physiol. Biochem. Zool.* **79**, 282–294 (2006).

52. M. B. Araújo, *et al.*, Heat freezes niche evolution. *Ecol. Lett.* **16**, 1206–1219 (2013).

53. J. Sunday, *et al.*, Thermal tolerance patterns across latitude and elevation. *Philos. Trans. R. Soc. Lond. B Biol. Sci.* **374** (2019).

54. L. B. Buckley, R. B. Huey, J. G. Kingsolver, Asymmetry of thermal sensitivity and the thermal risk of climate change. *Glob. Ecol. Biogeogr.* (2022). https://doi.org/10.1111/GEB.13570.

55. A. A. Hoffmann, S. L. Chown, S. Clusella-Trullas, Upper thermal limits in terrestrial ectotherms: How constrained are they? *Funct. Ecol.* **27**, 934–949 (2013).

56. J.-F. Arnoldi, A. L. Jackson, I. Peralta-Maraver, N. L. Payne, A universal thermal performance curve arises in biology and ecology. *Proc. Natl. Acad. Sci. U. S. A.* **122**, e2513099122 (2025).

57. J. J. Ruel, M. P. Ayres, Jensen's inequality predicts effects of environmental variation. *Trends Ecol. Evol.* **14**, 361–366 (1999).

58. T. L. Martin, R. B. Huey, Why "suboptimal" is optimal: Jensen's inequality and ectotherm thermal preferences. *Am. Nat.* **171**, E102-18 (2008).

59. A. S. Cicchino, C. K. Ghalambor, W. C. Funk, Linking critical thermal maximum to mortality from thermal stress in a cold-water frog. *Biol. Lett.* **19**, 20230106 (2023).

60. E. L. Rezende, L. E. Castañeda, M. Santos, Tolerance landscapes in thermal ecology. *Funct. Ecol.* **28**, 799–809 (2014).

61. J. Kingsolver, L. Buckley, Quantifying thermal extremes and biological variation to predict evolutionary responses to changing climate. *Philosophical Transactions - Royal Society of London, B* **372** (2017).

62. P. Amarasekare, R. M. Coutinho, The intrinsic growth rate as a predictor of population viability under climate warming. *J. Anim. Ecol.* **82**, 1240–1253 (2013).

63. K. Duffy, T. C. Gouhier, A. R. Ganguly, Climate-mediated shifts in temperature fluctuations promote extinction risk. *Nat. Clim. Chang.* **12**, 1037–1044 (2022).

64. R. B. Huey, D. Berrigan, Temperature, demography, and ectotherm fitness. *Am. Nat.* **158**, 204–210 (2001).

65. Veritas Health Innovation, Melbourne, Australia., *Covidence systematic review software*.

66. J. C. Havird, *et al.*, Distinguishing between active plasticity due to thermal acclimation and passive plasticity due to Q10 effects: Why methodology matters. *Funct. Ecol.* **34**, 1015–1028 (2020).

67. A. S. Cicchino, *et al.*, Acclimation capacity of critical thermal maximum varies among populations: Consequences for estimates of vulnerability. *Ecosphere* **14**, 1–16 (2023).

68. L. Comte, J. D. Olden, Evolutionary and environmental determinants of freshwater fish thermal tolerance and plasticity. *Glob. Chang. Biol.* **23**, 728–736 (2017).

69. D. Padfield, H. O'Sullivan, S. Pawar, rTPC and nls.multstart : A new pipeline to fit thermal performance curves in r - SM. *Methods Ecol. Evol.* **12**, 1138–1143 (2021).

70. D. Padfield, G. Matheson, *nls.multstart* (2018).

71. *Bootstrap Methods and their Application* (Cambridge University Press, 1997).

72. A. Canty, B. D. Ripley, boot: Bootstrap R (S-Plus) Functions. (2021).

Acknowledgements

We thank Helen Vanos for logistical support. This study was the result of a working group supported by the Canadian Institute for Ecology and Evolution/ Institut Canadien d'Écologie et d'Évolution (ASC & JRB) and the University of Guelph Centre for Ecosystem Management (ASC & JB). This work was also supported by the Natural Sciences and Engineering Research Council of Canada (NSERC-PDF to ASC; NSERC Discovery Grant to JRB).

Data Availability

All data and code can be accessed from [zenodo link to github].

Author Contributions

Conceptualization: All authors
Methodology: All authors
Investigation: ASC, JC, JRB
Formal analysis: ASC, JRB
Validation: ASC, AR, JRB
Data Curation: ASC
Writing - Original Draft: ASC
Writing - Review & Editing: All authors
Visualization: ASC
Supervision: JRB
Project administration: ASC, JRB
Funding acquisition: ASC, JRB